IMPACT: International Journal of Research in
Engineering & Technology (IMPACT: IJRET)
ISSN 2321-8843
Vol. 1, Issue 5, Oct 2013, 57-68

IMPROVED EROSION RESISTANCE FOR THERMAL BARRIER CERAMIC COATING PROTECT

IBTIHAL A.MAHMOOD[1], WALAA W. JAMEEL[2] & LUBNA ALAA KHALEEL[3]

[1]Assistant Professor, Department of Mechanical Engineering, University of Technology, Iraq

[2]Lecturer, Technical College Baghdad Foundation of Technical Education, Iraq

[3]Technical College Baghdad Foundation of Technical Education, Iraq

ABSTRACT

The erosion wear resistance of Ni base super alloy (Monel 400) can be improved by thermal sprayed coatings produced by the high velocity oxygen fuel (HVOF). In this work, (Monel 400) is coated with two different types of coatings, the first one is Al_2O_{3+}5% TiO_2 and the second is Al_2O_3 +15% (7-8YSZ), these layers were made of 350-400 μm as top coat, pre-sprayed with 50-100 μm of 4NiCr5Al as a bond coat To study the erosion wear behavior of the coatings, erosion test apparatus was designed according to ASTM G-76 also a plan of experiments based on the Taguchi technique is used to acquire the erosion test data in a controlled way. An orthogonal array and signal-to-noise ratio are employed to investigate the influence of the coating materials, impingement angle and stand-off-distance on the erosion rate. The study reveals that the coating materials is the most significant factor influencing the erosion wear rate. Al_2O_3 +15% (7-8YSZ) has higher wear resistance than Al_2O_{3+}5% TiO_2, Porosity influences their performance when subjected to wear (loss of thickness increased as the porosity increased), The measurement of hardness before and after the wear tests indicates that there was no significant change in either the metal or the coated samples at 300^0C for 1 hr. To assess adherence index, porosity and the hardness for the Al_2O_3 +5% TiO_2 coating are 84%, 9% and 454 $HV_{0.3}$ respectively while for the Al_2O_3 +15% (7-8YSZ) coating are 80.1, 17% and483 HV $_{0.3}$ respectively.

KEYWORDS: Sprayed Coatings, Erosive Wear, Flyash, Alumina-Titania, Alumina-Zirconia, Taguchi Technique

INTRODUCTION

Boiler tube failure is the number one source of forced outages in all power generation plants. Residual fuel oil contains sodium, vanadium and sulfur as impurities, the latter react together to form low melting point compounds known as ash which is cause erosion. It is estimated, that these plants lose approximately 6% of their power generation annually, due to boiler tube leaks – 23% of which is due to erosive wear [1]. The erosive wear is the main cause of failures in economizer boiler tubes as shown in figure 1. The study of the mechanisms of erosive wear is therefore extremely important in order to develop suitable solutions to minimize or even eliminate maintenance procedures of such equipment's. The erosion wear mechanisms involve the removal of material from a given surface due to the impact of solid particles [2]

Figure 1: Illustrate Economizer Boiler Tube in a Thermoelectric Power Plant, the Shiny Appearance of Upper Surface Suggested Greater Erosion at 90º Impingement Angle [3]

In order to meet the challenge of the rising cost of high performance materials, Surface coating techniques have recently attracted the attention of investigators worldwide [4]. Thermal barrier coatings (TBCs) are widely used for this applications. The TBCs are usually composed of a MCrAlY bond coat (M = Ni, Co) as an oxidation resistant layer also in order to enhance the bond strength and reduce the effect of thermal expansion coefficient mismatch between the top coat and the substrate alloy and yttria-stabilized zirconia (YSZ), Al_2O_3 and TiO_2 as a topcoat that provides thermal insulation toward metallic substrate.

The selection of thermal barrier coating materials is restricted by some basic requirements. These requirements are high melting point, no phase transformation between room temperature and operating temperature, low thermal conductivity, chemical inertness, thermal expansions match with the metallic substrate, good adherence to the metallic substrate and low sintering rate of the porous microstructure. So far, only a few materials have been found to basically satisfy these requirements [5].

Although much progress has been made in the development of new materials, there exists at present no single material which can withstand all the extreme operating conditions in modern technology. So that the combined properties of the composite system can satisfy a particular set of operating conditions [6].

Coatings based on alumina are a good alternative when wear resistance and chemical stability are the controlling factor. Alumina is hard but its main drawback is its brittleness [7, 8]. The addition of titanium oxide leads to a balanced equilibrium of properties maintaining enough hardness and increasing considerably the coating toughness. Titanium oxide has a lower melting point and plays a role of binding alumina grains to achieve coatings with a higher density and wear resistance coating. Zirconia shows only 50% of alumina's hardness but transformation toughening improves fracture resistance, that is overall toughness and bending strength are substantially higher than for alumina. The zirconia appears as a finely dispersed phase in the alumina matrix [9].

These coatings are usually applied by a thermal spray process because a very high temperature is required to melt the ceramic powder [9, 7].Coatings produced by HVOF spray have comparatively lower porosity, higher hardness and superior bond strength than many of the other thermal spraying methods such as plasma spraying [10].

Statistical methods can be employed for precise identification of significant control parameters for optimization. In recent years, the Taguchi experimental design technique has become a widely accepted methodology for improving performance output. This method consists of a plan of a minimal number of experiments with the objective of acquiring data in a controlled way, executing these experiments, and analyzing data, in order to obtain information about the behavior of a given process. One of the advantages of the Taguchi method over the conventional design of experiment (DOE) methods is that it minimizes the variability around the target when bringing the performance value to the target value in addition to keeping the experimental cost and time at the minimum level. Another advantage is that optimum working conditions determined from the laboratory work can also be reproduced in the real production environment [11]. Precisely, Taguchi’s design is a simple, efficient, and systematic approach to optimize designs for performance, quality, and cost [12, 13]. Hence, in this work, the Taguchi experimental design method has been adopted to investigate the effects of the impingement angle, stand-off-distance and coatings materials on the erosion wear rate

Warwood et al [14] 2001: Emphasized the significant application of taguchi's experimental design industry because it is a powerful approach to optimize the performance of the process.

The results of the study by ***Antony et al [15] 1999***: Revealed the stimulus for the wider application of Taguchi's experimental design techniques in manufacturing companies to achieve process improvement and reduce variability.

S. P. Sahu et al. [1]2010: Studied the erosion wear behavior of metal(aluminum powder)–ceramic(fly ash) composite coatings deposited on metal(aluminum) substrates by plasma spraying, Solid particle erosion (silica sand) characteristics of these coatings have been successfully analyzed using Taguchi experimental design. Significant control factors affecting the erosion rate have been identified through successful implementation of this technique. Impact velocity, aluminum content and impingement angle in declining sequence are found to be significant for minimizing the erosion rate.

J. Vicenzi et al. [3] 2006: Studied three different HVOF sprayed coatings (WC–12Co, Cr3C2–NiCr and WC–CrC–Ni) were tested under high temperature (_310 _C) erosion by means of an apparatus that simulated real conditions. The results showed that under these tests conditions the WC–12Co coating worn about 18 times less than bare SAE 1020 steel (substrate).

EXPERIMENTAL WORK

Deposition of Coatings

The substrate material selected for the present study was a Nickel based super alloy (Monel 400) this alloy finds applications in boiler components. The chemical composition of the substrate material is presented in table 1. Specimens with dimensions of approximately (40mm X 30mm X10mm); they were cut from a plate to the required shape. The samples were prepared for spraying process by grit blasting and cleaning before applying coating material.

Table 1: Chemical Composition of Ni Base Supper Alloy (Alloy 400)

Elements / Materials	Ni %	Cu %	Fe %	Mn %	C %	Si %	S %	Other
Nominal Chemical Composition [16]	63.0 min	28.0-34.0	2.5	0.2	0.3	0.5	0.024	…
Actual Chemical Composition	64.4	32.61	2.44	0.189	0.234	0.481	0.018	…

Four types of commercial powders were selected: 4Ni Cr 5Al with (50-90µm) as bond coat, an 8% Yttria-Stabilized Zirconia (YSZ) type (Saint-Gobain USA), TiO_2type (GCC England), Al_2O_3 type (Panreac Spain) has been used for TBC coating. In order to produce particle composite, two types of coatings were produced by the high velocity oxygen fuel (HVOF) method which included: Alumina (Al_2O_3) + 15% Ytteria Stabilizer Zirconia (7-8YSZ), Alumina (Al_2O_3) +5% Titania (TiO_2) as top coat. Each type of this powders were sieved in range 10-45µm by using a sieve analyzer with microsieves. Two batches with different mixing ratio (wt/wt) were prepared. The selected ratio of alumina-titania powders were mixed in the laboratory ball mill for 4 h, also for alumina -zirconia to get a uniform mixture of powders.

The coating technique in this work is the flame spray method type (rototec 800). This apparatus consists of a chamber containing a flange to hold the specimen and an Oxy- Acetylene flame. The powder particles flow with the flame and is deposited on the specimen. The powder was supplied through a special tube in the flame gun. The surface of metal was cleaned and roughened using emery paper (p220) and grit-blasted using sand blast system with pressure (4-6) bar. Then, the grit-blasted substrates were cleaned using anhydrous ethanol alcohol and dried to 200 °C by a furnace for 30 min. The ceramic powder Al_2O_3 +5% $TiO_2$and /Al_2O_3+15%YSZ with particle sizes 10-45 µm and NiCrAl metal powder (bond coat) with particle sizes ranging from 50 to 90 µm were used.

The specimen is fixed on the flange to make 90° with the powder flame flow. Then, the cooling system (air compressor) is switched on to cool the specimen from behind and keep it from melting during spraying process.

The system is switched on and the flame is ignited. The flame holder is controlled manually. The bond powder required for the first layer is loaded into the hopper, and the specimen is heated to a suitable temperature around (300 °C) by the flame.

The coating process is started by moving a lever on the hopper to allow all the powder to flow through the hopper with the flame with a distance of about (20 cm) between the flame and the specimen. The previous step is repeated until 50 to 100 μm thickness of bond layer has been reached. The ceramic powder (required for the top coat) is then loaded and the same procedure of bond was also repeated until 350 to 400 μm thickness has been reached. The coating is heated to about 1500 °C for a suitable time to permit the adhesion for layers.

The temperature for bond coat and top coat is controlled by adjusting the distance between the flame and the specimen and the pressure of Oxy-Acetylene (about 1500 °C for bond layers and 2800 °C for the ceramic layers). The flame is withdrawn gradually away from the specimen to minimize thermal shock. To measure the thickness of coating layer after spraying process, Coating thickness gauge type (QuaNix1500 Germany) was used, Infrared thermometer was used to know the temperature of surface before spraying process and the temperature of the fusion after spraying process.

Characterization of As-Sprayed Coating

In accordance with EN10209, the test in European standard of adherence strength, the coated specimen was tested by the steel ball falling impact. The adhesion strength was judged according the relics of coating on the destroyed surface. For obtaining a percentage number for adherence index, the imaging of microstructure of the peeled surface after the adherence strength test for samples was done by using an optical microscope with a digital camera. Then, the microstructure images were processed using "Adobe Photoshop CS6" program and the adherence index was calculated using the "Image J" program.

The as-sprayed coating was examined porosity, porosity measurements were carried out using boiling water immersion method for open pores determination. The procedure is summarized as follows:

- Determination of the dry weight (W) in grams.
- Immersion the samples in distilled water and boiling for 2 hours.
- After cooling to room temperature, weighting the suspended sample in distilled water (W_S) in grams.
- Determination the weight of saturated specimen with water in air (W_P), after removing all drops of water from the surface.

From above procedure the following parameters can be obtained

Apparent porosity $$(P\%) = \frac{Volume \quad of \quad Open \quad Pores}{Volume \quad of \quad Specimen} \times 100 \quad (1)$$

The volume of specimen = W-W_S in cm^3 (2)

The volume of open pores = W-W_p in cm^3 (3)

- Erosion Test Apparatus and Test Procedure

In order to simulate real service conditions that occur in boiler tube of a thermoelectric power plant, an experimental apparatus was developed, as shown in the schematic diagram in Figure 2. Such device was developed according to the ASTM G-76 standard, the set up used in this study for the solid particle erosion wear test is capable of creating reproducible erosive situations for assessing erosion wear resistance of the coating samples. It consists of an air compressor, a gauge pressure, gun, an air particle mixing chamber, accelerating tube, thermocouple and heater. These particles impact the specimen which can be held at different angles with respect to the direction of erodent flow using a swivel and an adjustable sample clip.

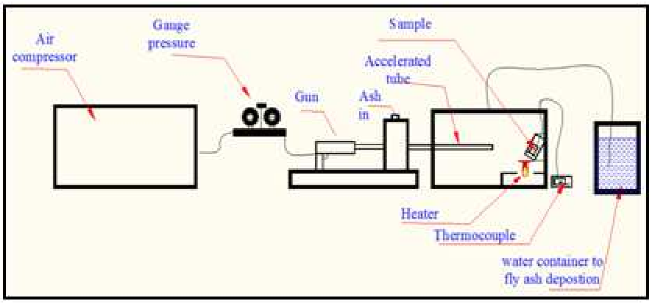

Figure 2: High Temperature Erosive Wear Apparatus Developed in this Work – Schematic

Fly ash used as erosive material, the characterization of the fly ash is given in Table2.

Table 2: Fly Ash Characterization

Chemical Composition	Sio_2: 31.86, Al_2O_3:25.12, Fe_2O_3:10.3
Morphology	Particles and Agglomerates Rounded and Angular Shapes

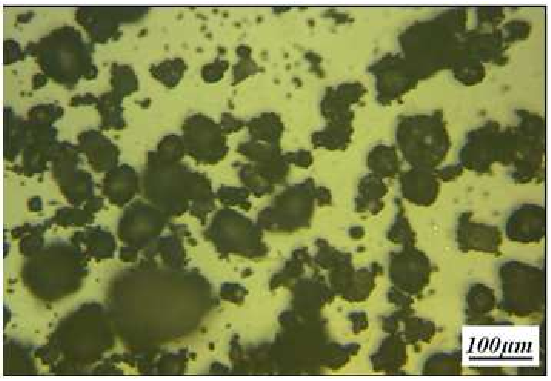

Figure 3: Morphology of Ash: Particles and Agglomerates Rounded and Angular Shapes

Establish and measure the particle velocity and particle flow specified. Adjust the pressure by use gauge pressure in order to obtain proper velocity of the eroding particles that is measured with a Digital anemometer instrument model DA40 also particle flow rate before inserting test specimens. Particle flow rate values are determined by collecting and subsequently weighing the abrasive exiting from the nozzle for a measured time period. Prepare the without coating specimen surface to achieve uniformity and adequate finish. Grinding through a series of abrasive papers to 400 grit is usually adequate so long as all surface scale is removed.

This test method utilizes a repeated impact erosion approach involving a small nozzle delivering a stream of gas containing abrasive particles which impacts the surface of a test specimen. The samples are cleaned carefully, dried and weighed to an accuracy of ± 0.01 mg using a precision electronic balance. Mount the specimen in proper location and orientation in the apparatus. Subject the specimen to particle impingement for a selected time interval. Remove the specimen, clean carefully, reweigh and calculate the weight loss The weight loss is recorded for subsequent calculation of erosion rate.

The process is repeated till the erosion rate attains a constant value called steady state erosion rate. Plot those values as weight loss versus elapsed time, and then the ratio of this weight loss to the weight of the eroding particles causing the loss is then computed as a dimensionless incremental erosion rate.

Parametric Appraisal and Taguchi Experimental Design

Statistical methods are commonly used to improve the quality of a product or process. Such methods enable the user to define and study the effect of every single condition possible in an experiment where numerous factors are involved. Solid particle erosion is such a process in which a number of control factors collectively determine the performance output, i.e., the erosion rate. In this context, Taguchi experimental design happens to be a powerful analysis tool for modeling and analyzing the influence of control factors on performance output.

This method achieves the integration of design of experiments (DOE) with the parametric optimization of the process yielding the desired results. The orthogonal array (OA) requires a set of well-balanced (minimum experimental runs) experiments.

Taguchi's method uses a statistical measure of performance called signal-to-noise ratio (S/N), which is logarithmic function of desired output to serve as objective functions for optimization. The ratio depends on the qualitative characteristics/attributes of the product/process/experimental variables to be optimized. The three categories of S/N ratios that are used are lower- the-better (LB), higher-the-better (HB) and nominal-the-best (NB). The S/N ratio for minimum erosion rate (ER) falling under smaller-the-better.

Table 3: Setting of Parameters

<table>
<tr><th>Control Factors</th><th>Symbols</th><th colspan="2">Fixed Parameters</th></tr>
<tr><td rowspan="8">Coating materials
stand-off distance
Impingement angle</td><td rowspan="8">Factor A
Factor B
Factor C</td><th>Erodent</th><th>fly Ash</th></tr>
<tr><td>Erodent feed rate (g/min)</td><td>6.5 ± 0.5</td></tr>
<tr><td>Test temperature ^{0}C</td><td>300</td></tr>
<tr><td>Nozzle diameter (mm)</td><td>6±0.075</td></tr>
<tr><td>Length of nozzle (mm)</td><td>150</td></tr>
<tr><td>Impact Velocity (m/s)</td><td>30</td></tr>
<tr><td>Test duration (min)</td><td>60</td></tr>
<tr><td>Pressure (kPa)</td><td>140</td></tr>
</table>

Table 4: Levels of the Variables Used in the Experiment

Parameter Code	Levels	
	I	II
Coating Materials	AT	AZ
Impingement Angle(Degree)	30	90
Stand-Off Distance(Mm)	50	80

Table 5: Orthogonal Array for L4 (2^3) Taguchi Design

Expt No	A	B	C
1	1	1	1
2	1	2	2
3	2	1	2
4	2	2	1

The most important stage in the design of experiment lies in the selection of the control factors. [13]. In the present work the impact of these three parameters are studied using L4 (2^3) orthogonal design. In conventional full factorial experiment design, it would require $2^3 = 8$ runs to study three factors each at two levels, whereas, Taguchi's factorial experiment approach reduces it to only 4 runs offering a great advantage in terms of experimental time and cost. The operating conditions under which erosion tests are carried out are given in Table 3. Different control factors and their selected levels are given in Table 4.

The tests are conducted as per experimental design given in Table 5 in which each column represents a test parameter whereas each row stands for a treatment or test condition corresponding to a combination of parameter levels, i.e., multi-parametric response whose output is presented in terms of erosion rates and S/N values. The plan of the experiments is as follows: the first column is assigned to coating materials (A), the second column to stand-off distance (B), the third column to impingement angle (C).

RESULTS AND DISSCUSIONS

- Characterization of As-Sprayed Coating

Alumina titania and alumina zirconia specimens have different in some properties as shown in table

Table 6: Illustrate Comparison between Al_2O_{3+}5% Tio_2 and Al_2O_3 +15% (7-8YSZ) Coating Properties

Coating Materials / Properties	Al_2O_3 +15% (7-8YSZ)	Al_2O_{3+}5% Tio_2
Hardness $(HV)_{0.3}$	483	454
Porosity %	17	9
Adherence Index (%)	80.1	84

Erosion Test

Figures 4, 5, 6 and 7 shows the weight loss due to erosion wear for the same impact velocity but at different coating materials, stand-off distance and impingement angle. In general erosion wear for the ceramic material is always less than that for the metal material for all conditions. These figures show the weight loss due to erosion wear increase in ceramic and in metal alloy with the running time. But the rate of weight loss of ceramic is always less than that of the metal alloy, because of the difference in melting point temperature and hardness. The erosion wear behavior of engineering materials can be grouped into ductile and brittle categories. It is known that impingement angle is one of the most important parameters in the erosion process and for ductile materials the peak erosion normally occurs at 15–20^0 angle while for brittle materials the erosion damage is maximum usually at normal impact, i.e., at 90^0 impingement angle.

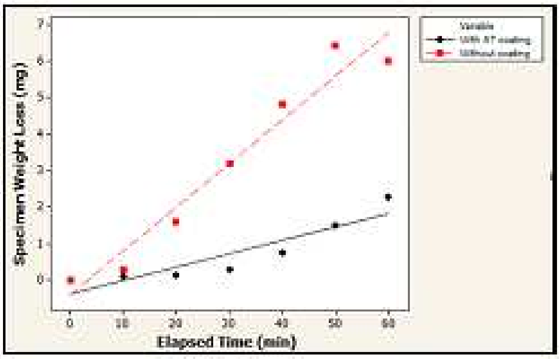

Figure 4: The Weight Loss Due to High Temperature Erosive Wear of Ceramic (Alumina-Titania) and Monel Alloy at Stand-off Distance 50mm, 30^0 Impingement Angle and Impact Velocity 30m/S

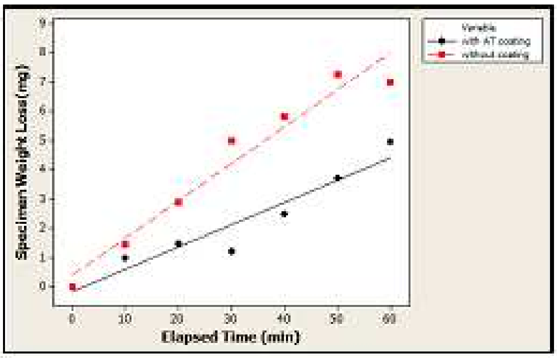

Figure 5: The Weight Loss Due to High Temperature Erosive Wear of Ceramic (Alumina-Titania) and Monel Alloy at Stand-off Distance 80mm, 90^0 Impingement Angle and Impact Velocity 30m/S

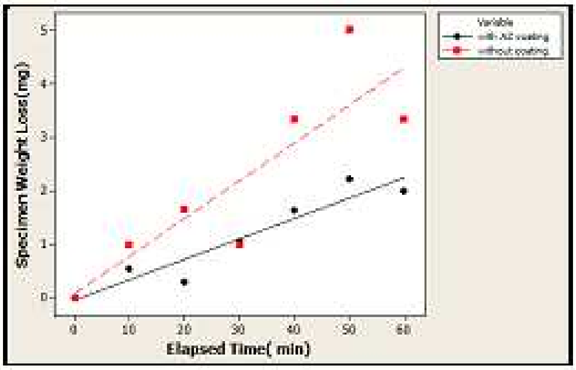

Figure 6: The Weight Loss Due to High Temperature Erosive Wear of Ceramic (Alumina-Zirconia) and Monel Alloy at Stand-off Distance 80mm, 30^0 Impingement Angle and Impact Velocity 30m/S

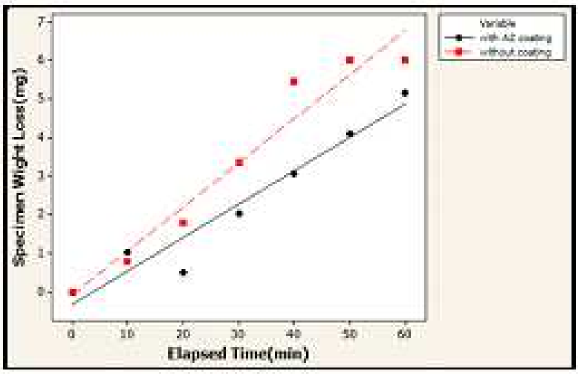

Figure 7: The Weight Loss Due to High Temperature Erosive Wear of Ceramic (Alumina-Zirconia) and Monel Alloy at Stand-off Distance 50mm, 90^0 Impingement Angle and Impact Velocity 30m/S

Analysis of Control Factor and Interaction

Table 7 Shows the experimental lay out and Table 8 shows the results with calculated S/N ratios for erosion wear rate of the coatings. Analysis of the influence of each control factor on the erosion is made with a signal-to-noise (S/N) response table, using MINITAB computer package. The response data of the testing process is presented in Table 9. The influence of control factors is also analyzed in the response table.

The control factor with the strongest influence is determined by differences values. The higher the difference, the more influential is the control factor. The strongest influence on erosion is found out to be coating materials (A) followed by impingement angle(C) and stand-off distance (B) respectively. It can also be concluded in Figure 8 illustrates this relative significance of control factors on the erosion wear rate.

Table 7: Experimental Lay out and Erosion Wear Rate Values

Run Number	Coating Materials	Stand-off Distance(Mm)	Impingement Angle(Degree)	Erosion Rate(Mg/Kg)
1	AT	50	30	12
2	AT	80	90	9.5
3	AZ	50	90	16
4	AZ	80	30	19

Table 8: Erosion Rate Values and The S/N Ratios

Run Number	Erosion Rate(mg/Kg)	S/N Ratio
1	**12**	-21.5836
2	**9.5**	-19.5546
3	**16**	-24.0824
4	**19**	-25.5751

Parameter A at level 1 = -21.5836+-19.5546*/2=-20.5691*

Parameter A at level2 = -24.0824+-25.5751/2=-25.19955

Parameter B at level1 = -21.5836+ -24.0824/2=-22.833

Parameter B at level2 = -19.5546+-25.5751/2=-22.56485

Parameter Cat level 1 = -21.5836+-25.5751/2=-23.57935

Parameter C at leve2 = -19.5546+-24.0824/2=-21.8185

Difference Δ (max-min)

Parameter A **=** (-20.5691--25.19955) =4.63045

Parameter B = (-22.56485--22.833) =0.26815

Parameter C = (-21.8185--23.57935) =1.76085

Table 9: The S/N Response Table for Erosion Rate

Level	A	B	C
1	**-20.5691**	**-22.833**	**-23.57935**
2	-25.19955	**-22.56485**	**-21.8185**
Diff	**4.63045**	**0.26815**	**1.76085**
Rank	**1**	**3**	**2**

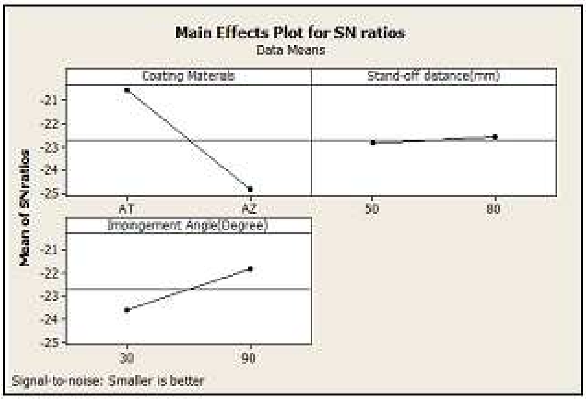

Figure 8: Effect of Control Factors on Erosion Rate

Figure 9 and 10 Shows the Samples Before and After the High Temperature Erosive Wear Test

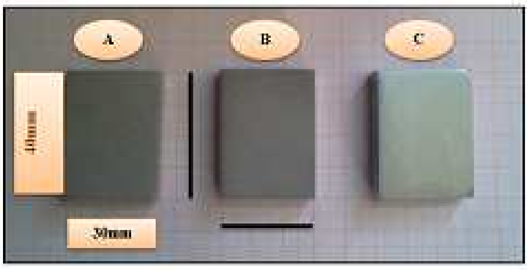

Figure 9: Photograph of Specimens before Erosion Wear Test A: with AT Coating B: with AZ Coating C: without Coating

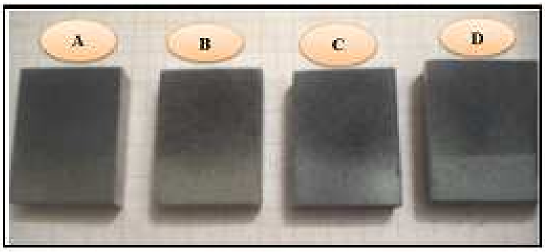

Figure 10: Photograph of Specimens after Erosion Wear Test A: AZ, 80mm, 30^0 B: AZ, 50mm.90^0 C: AT, 50mm, 30^0 D: AT 80 Mm, 90^0

Erosion Test Effect on Coating Layer Thickness

Also erosion wear of the samples may be evaluated by the decrease in thickness in the center of the specimens, which is the region more subjected to wear. Differences in thickness of the worn region in relation to the unworn region were used to quantify the loss of material from the coatings; the loss of thickness caused by erosive wear on the samples is shown in Figure 11. However, the erosion mechanism in the coatings is not well established, because some microstructure characteristics, like porosity, grain size, cracks influence their performance when subjected to wear. Table10 shows some properties of the coatings, including porosity and loss of thickness; it indicates that the loss of thickness increased as the porosity increased.

Table 10: Porosity Effect on Loss of Thickness of the Samples

Coating Materials	Porosity	Loss of Thickness(μm)
1- AT, 50mm, 30^0	low	15
2- AT, 80mm, 90^0	low	23
3- AZ, 50mm, 90^0	high	33
4- AZ, 80mm, 30^0	high	20

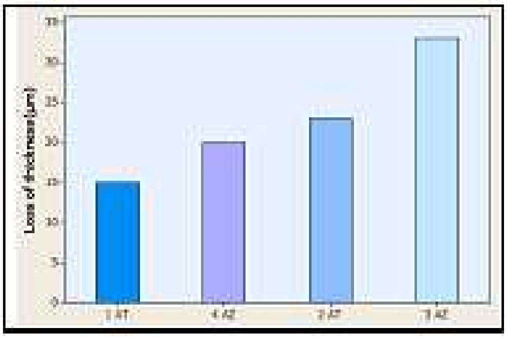

Figure 11: Loss of Thickness of the Samples Due to Erosive Wear

Erosion Test Effect on Coating Layer Microhardness

To evaluate whether the samples underwent microstructural changes in response to the test temperature (300 ^{0}C) and exposure time (1 h), their hardness were measured before and after the wear tests (see table 11). An analysis of the results indicates that there was no significant change in either the metal or the coated samples. Hence, it can be inferred that this temperature and/or time were not enough to modify the microstructures or even to relieve the pre-existing stresses or stresses generated during the test

Table 11: Microhardness before and after Erosive Wear Tests

Materials	Microhardness HV $_{0.3}$	
	Before Erosion Wear	After Erosion Wear
Ni base supper alloy	235	258
1- AT, 50mm, 30^0	454	462
2- AT, 80mm, 90^0	454	466
3- AZ, 50mm, 90^0	483	498
4- AZ, 80mm, 30^0	483	493

CONCLUSIONS

Two types of ceramic composite coating were prepared by using mixtures of Al_2O_{3+}5% TiO_2 and the other type Al_2O_3 +15% (7-8YSZ). The coatings were HVOF-sprayed onto Monel 400 substrate pre-sprayed with 4NiCr5Al layer. The system studied and the flowing conclusions were made.

- Solid particle erosion characteristics of these coatings have been successfully analyzed using Taguchi experimental design. Significant control factors affecting the erosion rate have been identified through successful implementation of this technique. Coating materials, impingement angle and stand-off distance in declining sequence are found to be significant for minimizing the erosion rate.
- Porosity and hardness of Al_2O_3 +15% (7-8YSZ) is more than Al_2O_{3+}5% TiO_2
- Adherence index of Al_2O_{3+}5% TiO_2 is more than Al_2O_3 +15% (7-8YSZ).
- Al_2O_3 +15% (7-8YSZ) has higher wear resistance than Al_2O_{3+}5% TiO_2
- Porosity influences their performance when subjected to wear (loss of thickness increased as the porosity increased).
- The measurement of hardness before and after the wear tests indicates that there was no significant change in either the metal or the coated samples

REFERENCES

1. Suvendu Prasad Sahu, Alok Satapathy, Amar Patnaik, K. P. Sreekumarand P. V. Ananthapadmanabhan, "Development, characterization and erosion wear response of plasma sprayed fly ash-aluminum coatings", Materials and Design, Vol.31, 2010, pp .1165–1173.
2. Hutchings IM. "The erosion of ductile metals by solid particles" PhD. Dissertation, University of Cambridge 1974, pp. 45–52.
3. J. Vicenzi, D. L. Villanova, M. D. Lima, A. S. Takimi, C. M. Marques, C. P. Bergmann," HVOF-coatings against high temperature erosion (~300 °C) by coal fly ash in thermoelectric power plant", Materials and Design, Vol.27, 2006, pp236–242.
4. M.H. Li, X.F. Sun, J.G. Li, Z.Y. Zhang, T. Jin, H.R. Guan, and Z.Q. Hu: Oxid. Met., vol. 59, 2003, pp. 591–605.
5. H.D. Steffens, Kaczmark, Weld. World, Vol. 28, 1990, p224.
6. R.L. Jones, J. Am. Ceram. Soc., Vol. 75, No.7, 1992 p. 1818.
7. S.V. Joshi, M.P. Srivastava, Surf. Coat. Technol, Vol. 56, 1993p. 215.
8. Q.L. Ge, T.C. Lei, J.F. Mao, Y. Zhou, J. Mater. Sci. Lett., Vol .12, 1993 p819.
9. Y. A. Perera Mercado; "Diamond-Like Carbon and Ceramic Materials as Protective Coatings Grown by Pulsed Laser Deposition"; Ph.D. Thesis, Institute of Technology, ACHEN, Germany (2003).
10. Metals Handbook, ASM, Metals Park, OH, Vol. 10, 1975.
11. Sahin Y. "The prediction of wear resistance model for the metal matrix composites". Wear, Vol .22, 2005, pp.258-1717.
12. Prasad BK, Das S, Jha AK, Modi OP, Dasgupta R, Yegneswaran AH." Factors controlling the abrasive wear response of a zincbased alloys silicon carbide particle composite." Composites: Part A, Vol .28A, No.8, 1997, p.301.
13. Phadke MS. "Quality engineering using robust design". AT&T, Bell Laboratories report. NJ: Prentice-Hall International Editions; 1989.
14. Warwood, S.Antony, J.Kiran, F.and Rowlands, H., "Process optimization using Taguchi methods of experimental design work study, MCB university prss, Vol.50, No.2, 2001, pp.51-57.
15. Antony, J.Hughes, M., & Kaye, m., "Reducing manufacturing process variability using experimental design technique: A case study", integrated manufacturing system MCB university press , Vol.10, No.3, 1999, pp.162-169.
16. Metals Handbook, ASM, “Properties and Selection: Nonferrous Alloys and Special-Purpose Materials”. Metal Park OH, USA., Vol.2 , 1990 , p. 271 .